Electronic Supplementary Material (ESI) for Dalton Transactions.
This journal is © The Royal Society of Chemistry 2022

ELECTRONIC SUPPLEMENTARY INFORMATION

NIR luminescence thermometers based on Yb-Nd coordination compounds in the 83-393K temperature range

Anastasia V. Orlova [a], Vladislava Yu. Kozhevnikova [a], Leonid S. Lepnev [b], Alexander S. Goloveshkin [c] and Valentina V. Utochnikova [a]

a. *a. M.V. Lomonosov Moscow State University 1/3 Leninskye Gory, Moscow, 119991, Russia*
b. *P.N. Lebedev Physical Institute, Russian Academy of Sciences, Leninsky prosp. 53, Moscow, 119992, Russia*
c. *A. N. Nesmeyanov Institute of Organoelement Compounds, Russian Academy of Sciences, Vavilova St. 28, 119991 Moscow, Russian Federation*

Contents

Experimental Section

Materials and methods

All solvents and chemicals were purchased from commercial sources.

X-ray powder diffraction (XRD) measurements were performed on Bruker D8 Advance Vario diffractometers (λ(CuKα1) = 1.54046 Å, Ge (111) monochromator, position-sensitive detector LynxEye, θ/2θ geometry, with rotation).

Thermal analysis was carried out on a thermoanalyzer STA 449 F1 Jupiter (NETZSCH, Germany) in the temperature range of 40–1000 °C in air, heating rate 10 °/min. The evolved gases were simultaneously monitored during the TA experiment using a coupled QMS 403 Aeolos quadrupole mass spectrometer (NETZSCH, Germany). The mass spectra were registered for the species with following m/z values: 18 (corresponding to H_2O), 28 (corresponding to N_2) and 44 (corresponding to CO_2).

Elemental analysis was performed on a Carlo Erba Elemental Analyzer 1106.

The IR spectra were recorded on an Thermo Scientific™ Nicolet™ iS50 FTIR Spectrometer as powdered at ATR.

X-ray microanalysis was carried out on a Leo Supra 50 VP scanning electron microscope equipped with an INCA Energy + Oxford 350X-Max 80 X-ray energy dispersion spectrometer. Measurements were made for each sample both at the point and in area. **Absorption spectra** were recorded in the range 200-800 nm using Perkin-Elmer Lambda 650 spectrometers to determine the maximum absorption of the ligand, as well as to estimate the molar extinction coefficient of the ligand.

Emission spectra and lifetimes were measured using Edinburgh Instruments FLS980 Fluorescence Spectrometer equipped with 450 W Xenon lamp, diode laser (λ_{ex} = 365 nm) for spectra and nitrogen laser (λ_{ex} = 337 nm) for lifetimes and Hamamatsu R928P PMT detector.

Photoluminescence quantum yield were determined using a diode laser (λ_{ex} = 365 nm) as an excitation source with Ocean Optics Maya 2000 spectrometer upon excitation with a xenon lamp at 25 °C. According to absolute modified de Mello et al. [38] method we carried out measurements in an integration sphere and calculated it by formula (4), when (i) L_a is the integrated intensity of Rayleigh scattering band (measurement at the excitation wavelength with empty cuvette in the sphere); (ii) L_c is the same integrated intensity at the excitation wavelength when the sample is introduced into the cuvette; (iii) E_a is the integrated intensity of the entire emission spectrum of empty cuvette; (iv) E_c is the integrated intensity of the entire emission spectrum of cuvette with the sample.

$$PLQY = \frac{E_c - E_a}{L_a - L_c} \cdot 100\% \qquad \textbf{(4)}$$

Synthesis of Ln(ant)$_3$

To a water solution of K(ant) (0.3 mmol, *in situ* from KOH and H(ant)), a water solution of $LnCl_3 \cdot 6H_2O$ (0.1 mmol; Ln = $Yb_xNd_yGd_{1-x-y}$) was added, resulting in the formation of lanthanide complex precipitate. Then the mixture was boiled for a few minutes for better crystallization, precipitate was separated by centrifugation, washed by distilled water to remove dissolvable precursors and by-products, and dried in air.

$Nd_{0.4}Gd_{0.6}$(ant)$_3$. Elemental analysis (%), calcd. for $Nd_{0.4}Gd_{0.6}(C_{15}H_9O_2)_3$ (815.5): C, 66.22; H, 3.31. Found: C, 66.93; H, 3.34.

$Yb_{0.2}Gd_{0.8}$(ant)$_3$. Elemental analysis (%), calcd. for $Yb_{0.2}Gd_{0.8}(C_{15}H_9O_2)_3$ (823.9): C, 65.55; H, 3.28. Found: C, 65.02; H, 3.25.

Synthesis of Ln(acr)$_3$(H$_2$O)$_8$

To a water solution of K(acr) (0.3 mmol, *in situ* from KOH and H(acr)·H_2O), a water solution of $LnCl_3 \cdot 6H_2O$ (0.1 mmol; Ln = $Yb_xNd_yGd_{1-x-y}$) was added, resulting in the formation of lanthanide complex precipitate. Then the mixture was boiled for a few minutes for better crystallization, precipitate was separated by centrifugation, washed by distilled water to remove dissolvable precursors and by-products, and dried in air.

$Yb_{0.2}Gd_{0.8}(acr)_3(H_2O)_8$. Elemental analysis (%), calcd. for $Yb_{0.2}Gd_{0.8}(C_{14}H_8NO_2)_3(H_2O)_8$ (970.4): C, 51.94; N, 4.33; H, 4.12. Found: C, 51.77; N, 4.44; H, 4.45.

$Yb_{0.5}Gd_{0.5}(acr)_3(H_2O)_8$. Elemental analysis (%), calcd. for $Yb_{0.5}Gd_{0.5}(C_{14}H_8NO_2)_3(H_2O)_8$ (906.3): C, 55.61; N, 4.63; H, 4.41. Found: C, 55.95; N, 4.61; H, 4.52.

$Nd_{0.3}Gd_{0.7}(acr)_3(H_2O)_8$. Elemental analysis (%), calcd. for $Nd_{0.3}Gd_{0.7}(C_{14}H_8NO_2)_3(H_2O)_8$ (963.4): C, 52.32; N, 4.36; H, 4.15. Found: C, 51.85; N, 4.48; H, 4.23.

$Nd(acr)_3(H_2O)_8$. Elemental analysis (%), calcd. for $Nd(C_{14}H_8NO_2)_3(H_2O)_8$ (954.24): C, 52.82; N, 4.40; H, 4.19. Found: C, 52.22; N, 4.35; H, 4.18.

$Yb_{0.1}Nd_{0.1}Gd_{0.8}(acr)_3(H_2O)_8$. Elemental analysis (%), calcd. for $Yb_{0.1}Nd_{0.1}Gd_{0.8}(C_{14}H_8NO_2)_3(H_2O)_8$ (963.4): C, 52.07; N, 4.34; H, 4.13. Found: C, 52.37; N, 4.50; H, 4.16.

TGA data

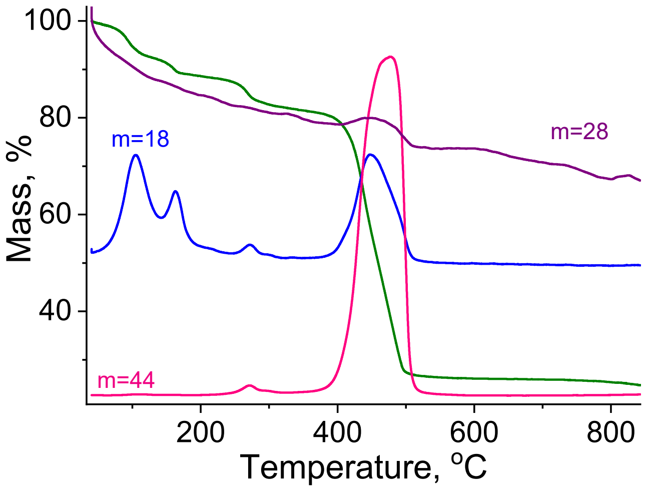

Figure S1. TGA-data for $Yb_{0.4}Gd_{0.6}(acr)_3(H_2O)_n$

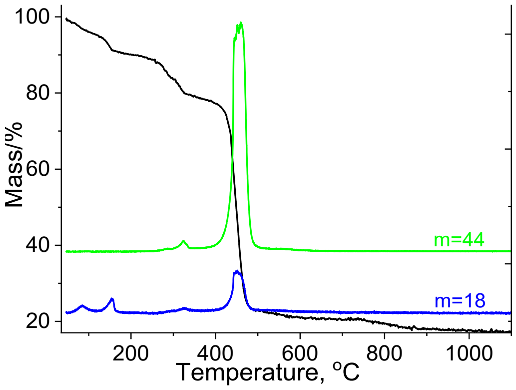

Figure S2. TGA-data for $Yb_{0.05}Nd_{0.45}Gd_{0.5}(acr)_3(H_2O)_n$

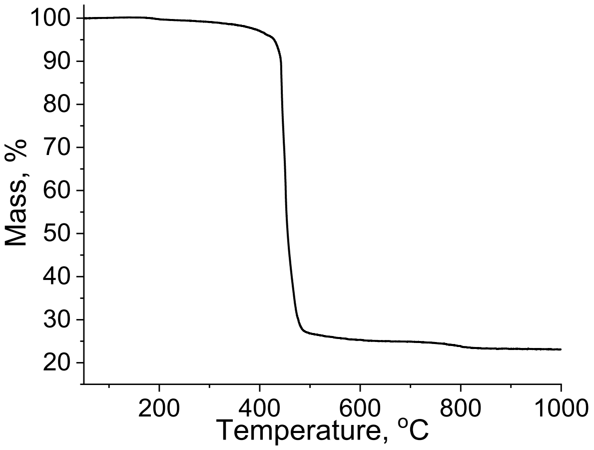

Figure S3. TGA-data for $Nd_{0.12}Yb_{0.02}Gd_{0.86}(ant)_3$

IR-spectroscopy

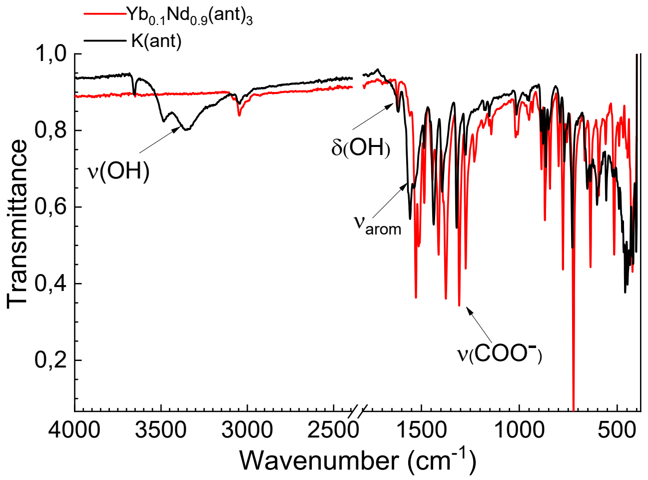

Figure S4. IR-spectroscopy data for $Yb_{0.1}Gd_{0.9}(ant)_3$

Triplet statement measurement

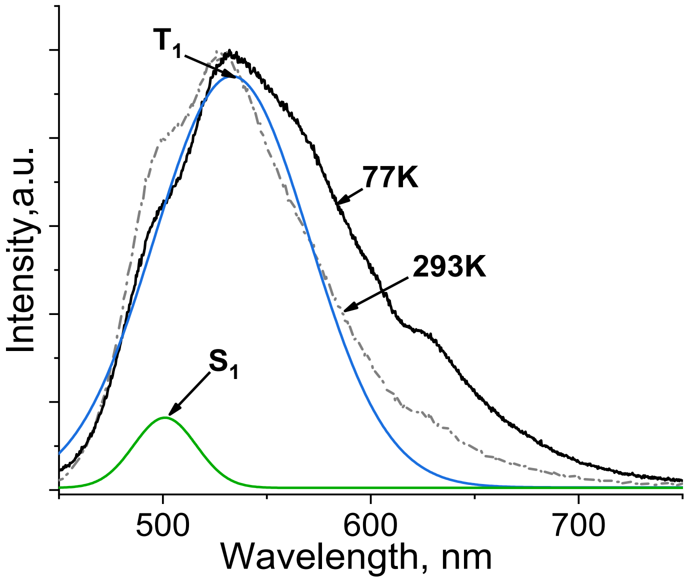

Figure S5. Luminescence spectra of $Gd(acr)_3(H_2O)_n$ at 77 and 293K

EDX data

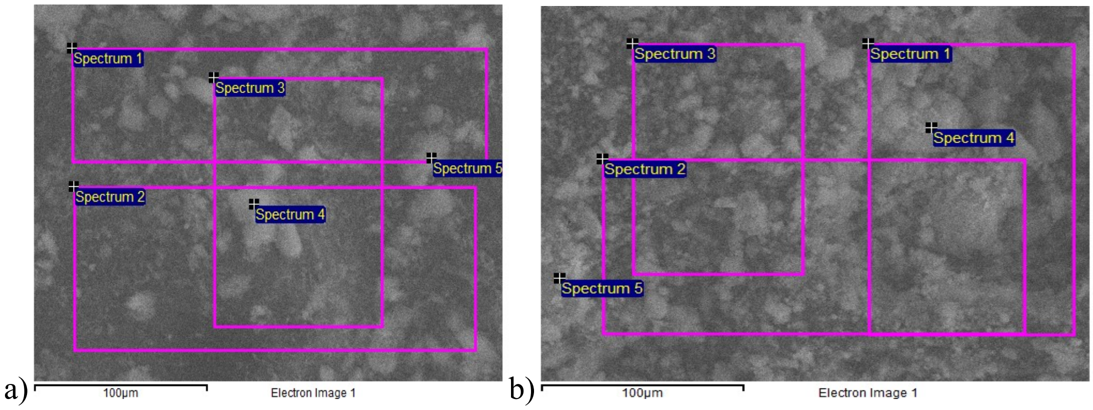

Figure S6. EDX element mapping for a) $Yb_{0.02}Nd_{0.14}Gd_{0.86}(ant)_3$ b)$Yb_{0.1}Nd_{0.1}Gd_{0.8}$ $(acr)_3(H_2O)_n$

Table S1. EDX data

Sample	Theoretical Yb fraction, %	Theoretical Nd fraction, %	Obtained Yb fraction, %	Obtained Nd fraction, %
$Yb_{0.1}Gd_{0.9}(ant)_3$	10	-	10±1	-
$Yb_{0.2}Gd_{0.8}(ant)_3$	20	-	21±1	-
$Yb_{0.3}Gd_{0.7}(ant)_3$	30	-	32±1	-
$Yb_{0.4}Gd_{0.6}(ant)_3$	40	-	41±1	-
$Yb_{0.5}Gd_{0.5}(ant)_3$	50	-	52±1	-
$Nd_{0.1}Gd_{0.9}(ant)_3$	-	10	-	9±1
$Nd_{0.2}Gd_{0.8}(ant)_3$	-	20	-	20±1
$Nd_{0.3}Gd_{0.7}(ant)_3$	-	30	-	31±1
$Nd_{0.4}Gd_{0.6}(ant)_3$	-	40	-	38±1
$Nd_{0.5}Gd_{0.5}(ant)_3$	-	50	-	49±1
$Yb_{0.1}Gd_{0.9}(acr)_3(H_2O)_n$	10	-	9±1	-
$Yb_{0.2}Gd_{0.8}(acr)_3(H_2O)_n$	20	-	22±1	-
$Yb_{0.3}Gd_{0.7}(acr)_3(H_2O)_n$	30	-	31±1	-
$Yb_{0.4}Gd_{0.6}(acr)_3(H_2O)_n$	40	-	39±1	-
$Yb_{0.5}Gd_{0.5}(acr)_3(H_2O)_n$	50	-	50±1	-
$Nd_{0.1}Gd_{0.9}(acr)_3(H_2O)_n$	-	10	-	10±1
$Nd_{0.2}Gd_{0.8}(acr)_3(H_2O)_n$	-	20	-	21±1
$Nd_{0.3}Gd_{0.7}(acr)_3(H_2O)_n$	-	30	-	30±1
$Nd_{0.4}Gd_{0.6}(acr)_3(H_2O)_n$	-	40	-	41±1
$Yb_{0.1}Nd_{0.1}Gd_{0.8}(acr)_3(H_2O)_n$	20	20	20±1	19±1
$Yb_{0.02}Nd_{0.12}Gd_{0.86}(ant)_3$	2	12	2±1	11±1

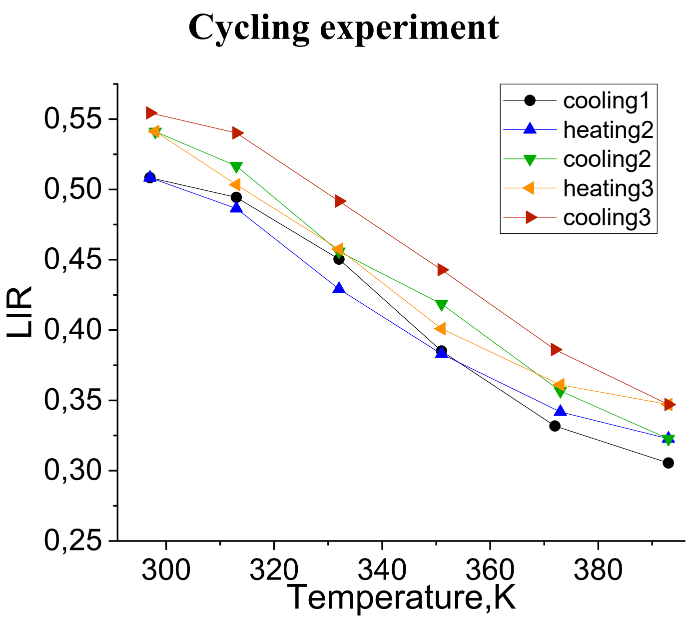

Figure S7. LIR of $Yb_{0.02}Nd_{0.12}Gd_{0.86}(ant)_3$ for series of heating and cooling experiments up to various temperatures

Thermometric parameters

Table S2. Thermometric parameters for $Yb_{0.02}Nd_{0.12}Gd_{0.86}(ant)_3$ at 77-293 K

$\mathbf{Yb_{0.02}Nd_{0.12}Gd_{0.86}(ant)_3}$ **at 77-293 K**		
Thermometric parameter	**Mathematical definition**	**Value**
Absolute sensitivity, $\mathbf{S_a}$	$S_a = \left\lvert\frac{}{dT}\right\rvert$	$0.0055K^{-1}$
Relative sensitivity, $\mathbf{S_r}$	$S_a = \left\lvert\frac{}{dT}\right\rvert * \frac{}{LIR} * 100\%$	$0.5\%K^{-1}$
Temperature resolution, **δT**	$\delta T = \frac{}{S_a}$	4K

Table S3. Thermometric parameters for $Yb_{0.1}Nd_{0.1}Gd_{0.8}(acr)_3(H_2O)_n$ at 77-293 K

$\mathbf{Yb_{0.1}Nd_{0.1}Gd_{0.8}(acr)_3(H_2O)_n}$ **at 77-293 K**		
Thermometric parameter	**Mathematical definition**	**Value**
ыыыAbsolute sensitivity, $\mathbf{S_a}$	$S_a = \left\lvert\frac{}{dT}\right\rvert$	$0.0015K^{-1}$
Relative sensitivity, $\mathbf{S_r}$	$S_a = \left\lvert\frac{}{dT}\right\rvert * \frac{}{LIR} * 100\%$	$0.17\%K^{-1}$
Temperature resolution, **δT**	$\delta T = \frac{}{S_a}$	15K

Table S4. Thermometric parameters for $Yb_{0.02}Nd_{0.12}Gd_{0.86}(ant)_3$ at 293-393 K

$\mathbf{Yb_{0.02}Nd_{0.12}Gd_{0.86}(ant)_3}$ **at 293-393 K**		
Thermometric parameter	**Mathematical definition**	**Value**
Absolute sensitivity, $\mathbf{S_a}$	$S_a = \left\lvert\frac{}{dT}\right\rvert$	$0.0022K^{-1}$
Relative sensitivity, $\mathbf{S_r}$	$S_a = \left\lvert\frac{}{dT}\right\rvert * \frac{}{LIR} * 100\%$	$1.8\%K^{-1}$
Temperature resolution, **δT**	$\delta T = \frac{}{S_a}$	1.5K

.

Approximation of the LIR temperature dependence for $Yb_{0.02}Nd_{0.12}Gd_{0.86}(ant)_3$

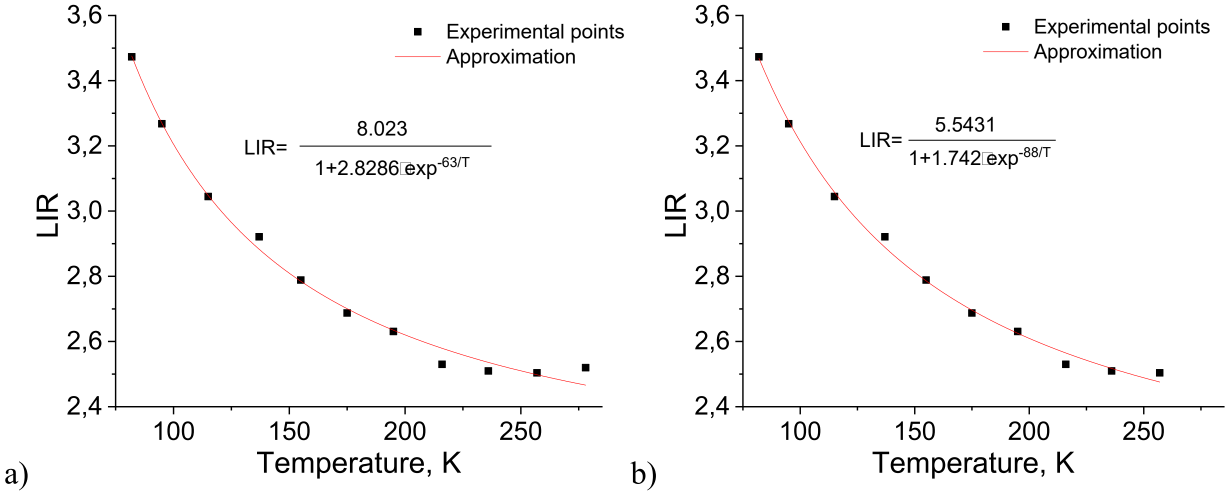

Figure S8. Theoretical LIR curve at a) 83-277K and b) 83-257K in approximation of three-level system

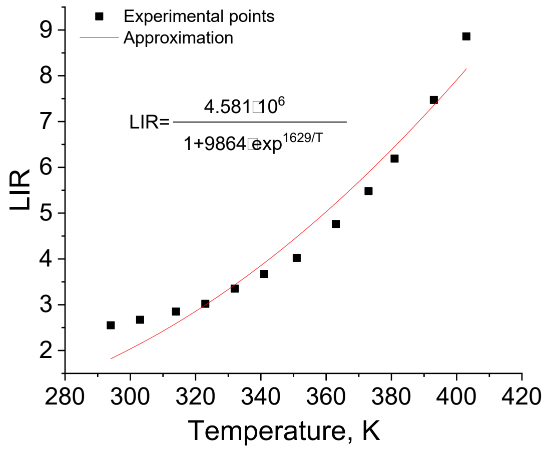

Figure S9. Theoretical LIR curve at 293-393K in approximation of three-level system

Table S5. The coefficients of the equation $LIR = \frac{B}{1 + A \cdot exp(\frac{E_a}{T})}$ and R^2 for various temperature ranges

Temperature range	A	B	E_a	R^2
Low temperature range (83-277 K)	8.02 ± 5.42	2.83 ± 2.50	63.23 ± 24.91	0.99307
Low temperature range without last point (83-257 K)	5.54 ± 1.06	1.74 ± 0.46	87.7 ± 19.5	0.99659
Low temperature range without last two points (83-237 K)	4.92 ± 0.57	1.50 ± 0.22	104.39 ± 18.9	0.99752
High temperature range (293-393 K)	$5.12 \pm 2.19 \cdot 10^{12}$	$11\,023 \pm 4.73 \cdot 10^{9}$	-1 629 ± 664	0.95405

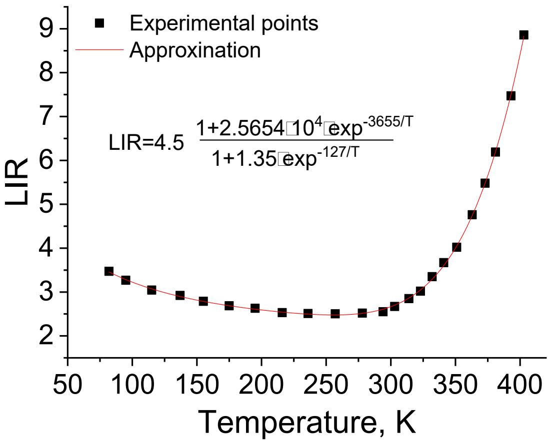

Figure S10. Theoretical LIR curve at 83-393K in approximation of four-level system